D2.1

Report on Process Modelling and Simulation of Hydrogen Production from Plastics

Hydrogen Production from Waste (HyWay)

Prof. Dr. Bradley P. Ladewig

Project number:	101130009
Work package:	WP2 — Simulation, modelling and digital twinning
Lead beneficiary:	University of Luxembourg (UL)
Deliverable type:	R — Document, report
Dissemination level:	PU — Public
Version:	Final
DOI:	10.5281/zenodo.2172194
Date:	July 31, 2026

Co-funded by the European Union

Funded by the European Union. Views and opinions expressed are, however, those of the author(s) only and do not necessarily reflect those of the European Union or the granting authority. Neither the European Union nor the granting authority can be held responsible for them.

Executive summary

Hydrogen production from waste plastics combines a difficult feedstock problem with a multi-scale reacting-system problem. Plastic mixtures melt, devolatilise and crack through strongly temperature-dependent pathways; vapours undergo secondary cracking, reforming and water–gas shift reactions; catalysts may deactivate through coke, sintering or contaminants; and reactor hydrodynamics control heat transfer, residence time and contact between phases. No single model resolves all of these phenomena at useful engineering scale.

This report reviews how the literature represents those coupled phenomena and organises available methods into four levels: thermodynamic bounds, kinetic and reactor-network models, reactor-scale computational fluid dynamics, and coupled or reduced multiscale models. It gives particular attention to open tools that support transparent equations, version-controlled inputs and execution on high-performance computing facilities. Candidate components include Cantera for thermochemistry and reacting networks, OpenFOAM and MFiX for continuum and particle-resolved reactor modelling, and Python-based scientific libraries, PETSc and SUNDIALS for parameter estimation, integration and scalable numerical solution.

The intended outcome is not a single universal model. It is a reproducible modelling hierarchy in which low-cost models screen feedstocks and operating conditions, higher-fidelity simulations interrogate transport and hydrodynamics, and all levels are tested against explicit experimental observables. A new open Cantera case study demonstrates the first level of that hierarchy. A 44,064-case equilibrium sweep was executed as 111 CPU job-array tasks on the University of Luxembourg Aion HPC system. It quantifies the effects of temperature, steam-to-carbon ratio, pressure and four idealised feed compositions. For the mixed feed, the sampled-grid maximum was 2.409 mol H_2 per mol feed carbon at 670 °C, 1 bar and S/C=4; however, this is a thermodynamic upper bound driven by excess steam rather than a kinetic reactor optimum. The calculation and the reviewed evidence together support low pressure, adequate steam and polymer-resolved feed descriptions as screening priorities, while confirming that kinetic and transport validation remain necessary.

Contents

List of Tables

List of Figures

Chapter 1

Introduction

1.1 Project and deliverable context

HyWay investigates routes for producing hydrogen-rich gas from waste. Within WP2, D2.1 addresses process modelling and simulation of hydrogen production from plastics. The deliverable is positioned between experimental studies of feedstock conversion and later work on higher-fidelity reactor simulation, data-driven modelling and model validation. This draft therefore treats the report as a critical review and modelling roadmap rather than as a claim that one model has already captured the complete process.

1.2 Problem statement

Waste-plastic conversion is challenging to model because the feed is neither a single chemical species nor a stable, homogeneous material. Polymer identity, additives, contamination, particle geometry and thermal history affect devolatilisation and product formation. At reactor scale, the heat required to melt and crack the feed must be transported through gas, liquid or softened polymer, solid residues and—in many designs—a circulating bed or catalyst. Hydrogen production then depends on downstream reactions of condensable and non-condensable products, particularly steam reforming and water–gas shift.

1.3 Aim and objectives

The report establishes an evidence-based foundation for open, reproducible modelling of plastic-to-hydrogen processes. Its objectives are to:

1. review established thermochemical routes from plastic waste to hydrogen-rich gas;
2. compare modelling assumptions, governing equations, data needs and validation practices reported in the literature;
3. assess open tools for thermodynamics, kinetics, reactor networks, multiphase CFD and particle methods;
4. examine how those tools can be deployed reproducibly on HPC systems;
5. define a staged modelling and validation strategy for HyWay;
6. demonstrate an executable, HPC-enabled equilibrium screening study.

1.4 Scope and boundaries

The primary feedstocks are polyethylene, polypropylene, polystyrene and representative mixed-plastic streams. PVC and PET are considered where their heteroatoms, corrosive products or oxygen content change modelling requirements. The main conversion chain comprises pyrolysis or

gasification, followed where relevant by catalytic cracking, steam reforming, water–gas shift and carbon-dioxide separation. The report focuses on process and reactor models; detailed economic, life-cycle and policy analyses remain interfaces to other HyWay work packages.

1.5 Structure of the report

Chapters 2–4 establish the review method, feedstock basis and conversion pathways. Chapters 5 and 6 analyse modelling approaches and published evidence. Chapter 7 assesses open tools, and Chapter 8 reports the HPC-enabled equilibrium study. Chapter 9 converts the combined literature and simulation evidence into recommendations for model development, validation and reproducibility.

Chapter 2

Review methodology

2.1 Review questions

The literature review is organised around five questions:

1. Which physical and chemical phenomena control hydrogen yield and gas composition from plastic feedstocks?
2. Which modelling fidelity is justified by the available measurements?
3. How transferable are reported kinetic parameters and product-lumping schemes across feedstocks and reactor types?
4. Which open tools can represent the required phenomena without hiding equations or property data?
5. What evidence is needed to regard a model as verified, validated and useful for prediction?

2.2 Search and selection strategy

The review combined database searches of journal literature with backward and forward citation tracing and official software documentation. Search concepts will combine plastic type or mixed-plastic waste with pyrolysis, gasification, reforming, hydrogen, kinetics, equilibrium, computational fluid dynamics, multiphase flow, discrete-element modelling, uncertainty and high-performance computing. A core set of 36 peer-reviewed primary studies was retained, supported by review literature and official software documentation. Recent reviews provide breadth, while primary experimental and modelling studies provide parameters, equations, boundary conditions and validation evidence [1].

2.3 Eligibility and evidence extraction

Studies were eligible when they reported a reproducible model of plastic conversion or of a directly relevant unit operation and provide sufficient information to identify inputs, outputs and modelling assumptions. Each study will be coded against the matrix in Table 2.1. Purely descriptive studies remain useful for process context but will not be treated as model-validation evidence.

2.4 Synthesis and quality assessment

Evidence was synthesised by model class rather than only by reactor type. Quality assessment distinguishes calibration from validation, records whether measurements are independent of parameter fitting, and identifies cases where agreement is achieved through unreported tuning.

Table 2.1: Evidence-extraction matrix for modelling studies.

Category	Information to extract
Feedstock	Polymer identity, mixture composition, additives, proximate and ultimate analysis, particle dimensions
Reactor	Configuration, scale, geometry, heating mode, catalyst and contacting pattern
Model	Fidelity, phases, governing equations, reaction network, closure relations and numerical method
Inputs	Thermophysical properties, kinetic parameters, boundary and initial conditions
Outputs	Conversion, yields, gas composition, temperature, pressure drop, residence time and spatial fields
Credibility	Code verification, grid/time-step independence, calibration method, validation data and uncertainty
Reproducibility	Software and version, source availability, case files, data, hardware and run configuration

Quantitative meta-analysis is unlikely to be defensible across all studies because product lumps and feedstocks differ; structured comparison and dimensionless analysis are more appropriate.

Chapter 3

Plastic feedstocks and conversion fundamentals

3.1 Polymer classes and mixed-waste composition

3.1.1 Polyethylene

Polyethylene is dominated by carbon–carbon and carbon–hydrogen bonds and typically decomposes through radical chain scission. Its high hydrogen-to-carbon ratio makes it a central reference feedstock, but melt behaviour and heat transfer complicate scale-up. Thermogravimetric and fixed-bed studies show that apparent kinetic parameters and product yields depend on heating history and bed thickness [2–4], while recent microwave work illustrates the additional coupling between field, temperature and product evolution [5].

3.1.2 Polypropylene

Branching changes bond environments and product distributions relative to polyethylene. Models must avoid treating all polyolefins as a single pseudo-component unless the consequences of that lumping are quantified.

3.1.3 Polystyrene

Polystyrene exhibits stronger depolymerisation behaviour and substantial aromatic product formation. A kinetic scheme suitable for polyolefins is therefore not automatically transferable. Two-stage experiments consistently show lower reformability or different catalyst response for PS than for polyolefins [6–8].

3.1.4 PET, PVC and heterogeneous mixtures

Oxygenated polymers alter gas and condensable composition, while chlorine from PVC introduces corrosion, catalyst-poisoning and emissions concerns. Mixed-plastic models need explicit composition bounds or probability distributions rather than a nominal “plastic” formula alone. Polymer-resolved experiments show that PE/PP-rich feeds generally yield more hydrogen than PS- or PET-rich feeds, while real mixtures occupy composition-dependent intermediate ranges [7–9].

3.2 Feedstock characterisation required by models

The minimum characterisation depends on model fidelity. Equilibrium and flowsheet-level balances may use elemental composition and heating value; kinetic models require polymer-resolved fractions and thermal-analysis data; particle and CFD models additionally require

density, heat capacity, thermal conductivity, phase-change behaviour, size distribution and radiative properties.

3.3 Thermal decomposition and product formation

3.3.1 Primary devolatilisation

Primary conversion links local temperature history to the release of gases, vapours and residue. Global one-step kinetics are computationally economical but may confound intrinsic chemistry with heat and mass transfer.

3.3.2 Secondary cracking and condensation

Vapour residence time and temperature influence secondary cracking, aromatisation and coke formation. Product definitions must remain consistent between experiments and models, especially where “oil”, “tar” and “condensables” are operationally defined.

3.3.3 Catalytic effects and deactivation

Catalysts change reaction pathways and can increase production of light gases or reform pyrolysis vapours. Models should represent activity loss when coke, contaminants or sintering materially change performance over the experimental time scale. Nickel preparation and zeolite support structure alter dispersion, pore accessibility, coke morphology and hydrogen yield [10, 11]; Fe–Ni synergy and waste-derived chars or ashes further show that catalyst identity cannot be reduced to metal loading alone [12–15].

3.4 Governing balances and performance indicators

At every fidelity, elemental closure is a non-negotiable diagnostic. For a control volume, total mass and elemental balances precede calculation of hydrogen yield, hydrogen selectivity, cold-gas efficiency or process efficiency. Reported indicators will be normalised to a clearly stated feed basis and accompanied by carbon and hydrogen closure wherever source data allow.

Chapter 4

Plastic-to-hydrogen conversion pathways

4.1 Pyrolysis as a feed-conversion stage

Pyrolysis produces a distribution of gas, condensable hydrocarbons and solid residue. It is best understood as the first stage of a hydrogen process rather than, by itself, a guarantee of high hydrogen yield. The modelling emphasis is on heat transfer, devolatilisation kinetics and the composition of vapours delivered to subsequent stages [2, 3]. Flash Joule heating offers a distinct high-rate route in which hydrogen and a graphitic carbon coproduct are produced together, but its allocation and scale-up assumptions differ from conventional steam reforming [16].

4.2 Gasification

4.2.1 Steam gasification

Steam provides a reactant for reforming and water–gas shift, but the outcome depends on temperature, steam-to-carbon ratio, residence time and catalytic surfaces. Experiments confirm that steam can shift production between hydrogen and deposited carbon, making both quantities necessary reporting outputs [17, 18].

4.2.2 Air and oxygen-blown gasification

Partial oxidation supplies heat internally but introduces nitrogen dilution with air and a trade-off between oxidation and hydrogen-rich product formation.

4.2.3 Carbon-dioxide-assisted conversion

Carbon dioxide can participate through dry reforming and gasification reactions. The approach is relevant to carbon management but introduces equilibrium, coking and catalyst-stability questions.

4.3 Pyrolysis coupled to catalytic steam reforming

A two-stage representation separates polymer decomposition from catalytic conversion of vapours. This structure is attractive for modelling because feed conversion and reforming can be calibrated against different measurements, while their coupling still preserves mass, energy and species flows. Continuous spouted-bed/fluidised-bed experiments demonstrate the value of this separation for pure and mixed feeds [7, 19], and a four-reaction reforming network with an explicit deactivation law has been fitted for HDPE pyrolysis volatiles [20].

4.4 Water–gas shift and carbon-dioxide separation

Water–gas shift redistributes carbon monoxide, steam, hydrogen and carbon dioxide. Separation or sorption can move the effective equilibrium but adds heat effects, capacity limits and cyclic behaviour that must be represented when they influence reported hydrogen performance.

4.5 Reactor configurations

4.5.1 Fixed and packed beds

Packed beds offer relatively simple geometry but may develop axial and radial temperature gradients, pressure drop and catalyst deactivation fronts.

4.5.2 Fluidised and circulating beds

Fluidised systems improve contacting and heat transfer but require closure for gas–solid momentum exchange, solids stresses, mixing and particle residence time.

4.5.3 Screw, rotary, microwave and plasma reactors

These systems impose distinct heat-transfer and electromagnetic or plasma physics. They should not be collapsed into a single generic reactor model without evidence that the omitted physics are secondary. Plasma-catalytic studies show material support, packing, catalyst and feed effects at low bulk temperature [21, 22], while photoreforming represents a separate aqueous, photocatalytic route outside the main thermochemical chain [23].

Chapter 5

Hierarchy of modelling approaches

5.1 Thermodynamic equilibrium

Equilibrium calculations provide limiting compositions and reveal the effects of temperature, pressure and elemental feed ratios. They are useful for screening and consistency checks, but do not predict finite-rate conversion, residence-time effects, hydrodynamic limitations or catalyst deactivation.

5.2 Kinetic models

5.2.1 Global and distributed-activation-energy models

Global models compact thermal-analysis data into a small number of rate expressions. Their parameters are often apparent rather than intrinsic and should not be transferred across heating rates, particle sizes and reactors without testing.

5.2.2 Lumped reaction networks

Lumped schemes balance chemical resolution and identifiability by grouping products into gas, liquid, wax, aromatic or solid fractions. Their utility depends on explicit lump definitions and sufficient independent measurements to constrain competing pathways.

5.2.3 Detailed and mechanistic chemistry

Detailed chemistry can represent secondary gas-phase and reforming reactions, but polymer decomposition produces a combinatorial species problem. A practical hierarchy may combine a reduced devolatilisation model with a more detailed gas-phase mechanism.

5.3 Zero- and one-dimensional reactor models

5.3.1 Batch and perfectly stirred reactors

Ideal reactors are useful for mechanism testing, parameter estimation and sensitivity analysis. They also create transparent baselines against which spatial models can be justified.

5.3.2 Plug-flow and axial-dispersion models

One-dimensional models capture residence-time development and axial heat or species variation at modest computational cost.

5.3.3 Networks of ideal reactors

Reactor networks can approximate staged equipment, bypass, recirculation and coupled pyrolysis–reforming systems. Network topology becomes a model assumption that should be tested against tracer or residence-time evidence.

5.4 Computational fluid dynamics

5.4.1 Single-phase reacting flow

Single-phase CFD is appropriate for reformers or gas-phase zones when solid or liquid feed conversion is supplied as a validated boundary condition or source term.

5.4.2 Eulerian–Eulerian multiphase models

Two-fluid models treat phases as interpenetrating continua. They are computationally tractable for large reactors but depend strongly on drag, granular stress, heat-transfer and reaction closures.

5.4.3 Eulerian–Lagrangian and CFD–DEM models

Particle tracking and DEM provide particle-scale histories and contact dynamics, at substantially higher computational cost. Coarse graining may be needed for engineering scale and introduces another validation target.

5.4.4 Particle-in-cell and coarse-grained approaches

MP-PIC and related methods occupy a useful middle ground between continuum solids and fully resolved DEM. Their smoothing and parcel assumptions must be reported alongside grid and parcel-independence studies.

5.5 Reduced-order and surrogate models

Reduced-order models and machine-learning surrogates can accelerate optimisation and uncertainty propagation after a trustworthy training domain has been established. They do not remove the need for conservation checks, out-of-domain detection and independent validation.

5.6 Multiscale coupling strategies

Coupling may be sequential, embedded or iterative. A defensible design states which information crosses each scale—for example kinetic rates, heat-transfer coefficients, residence-time distributions or source terms—and checks whether coupling errors exceed experimental uncertainty.

Chapter 6

Evidence from prior modelling studies

6.1 Kinetic studies of individual polymers

The primary pyrolysis literature spans conversion-only TGA models, lumped product networks and emerging multiscale approaches. LDPE TGA data can be fitted closely by isoconversional, model-fitting and neural-network methods [4], but a good mass-loss fit does not identify gas, liquid, wax and char pathways independently. The HDPE microbalance study of Al-Salem and Lettieri [2] adds product lumps, while the fixed-bed model of Li et al. [3] includes parallel primary reactions and secondary wax cracking. The strong bed-thickness dependence in the latter is direct evidence that apparent kinetics can embed heat and mass transfer. Microwave-assisted work combining experiments, atomistic simulation and product kinetics extends the evidence base, but introduces uncertainty in electromagnetic heating and temperature uniformity [5].

6.2 Mixed-plastic and real-waste models

Mixed-feed evidence does not support one universal plastic pseudo-component. Fast-pyrolysis and reforming experiments resolve clear differences among PE, PP, PS and PET [7]; plasma-catalytic tests with real post-consumer mixtures find intermediate behaviour controlled by composition [8]. Char-catalysed studies reach a similar feed ranking but also show why the catalyst-origin carbon must be included in the balance [9, 24]. Linear superposition of pure-polymer responses remains a useful baseline, but interaction terms or composition uncertainty are needed when mixture data depart from it.

6.3 Reactor-scale pyrolysis simulations

Reactor-scale models must distinguish prescribed volatile release from locally coupled conversion. Melting, particle shrinkage, radiation, bed depth and vapour-phase secondary reactions remain persistent scale-up challenges [1, 3]. Waste-derived ash studies additionally show that real inorganic matter can catalyse cracking and reforming, but its variable surface area, porosity and metals preclude a universal activity factor [13, 15]. These observations favour staged validation: first devolatilisation and heat transfer, then gas-phase conversion and catalytic effects.

6.4 Gasification and reforming simulations

The most directly reusable open-model pattern couples measured or modelled pyrolysis volatiles to an equilibrium or kinetic reformer. Cortazar et al. combined measured volatile compositions

with equilibrium oxidative steam reforming and explored temperature, steam/plastic ratio and equivalence ratio [25]. A complementary kinetic route uses reforming lumps for C_5^+, C_2–C_4, methane and water–gas shift, together with catalyst deactivation [20]; surrogate pyrolysis-oil and light-gas experiments provide additional compact kinetic targets [26, 27].

Process-level studies extend those units to gasification, shift, separation, heat recovery and carbon management. Aspen-based work has evaluated PE/PP gasification with added steam-methane reforming [28], PS/PP gasification with machine-learning surrogates [29], and restricted-equilibrium co-gasification of biomass and plastic [30]. Integrated studies quantify energy/exergy performance, industrial flowsheets and downstream product choices [31–33]. At system level, mixed-plastic gasification has been coupled to techno-economic, life-cycle and CCS analyses [34–36]. These models are useful boundary and flowsheet comparators, but they do not validate reactor kinetics merely by closing a plant balance.

Molecular simulations occupy the opposite end of the hierarchy. ReaxFF-MD and DFT calculations identify radical-assisted pathways in PE steam gasification [37]; they support mechanistic hypotheses but require reduction and experimental calibration before supplying reactor-scale rates. Across all fidelities, gas composition must be reported on its stated wet, dry, nitrogen-free or total basis.

6.5 Hydrodynamic and multiphase studies

The plastic-to-hydrogen literature contains far fewer public reactive CFD case files than equilibrium and flowsheet studies. Fluidised-bed experiments do, however, supply important validation targets: continuous contacting and feed mixing [7, 19], temperature and steam effects with sacrificial chars [14, 24], and recent fluidised-bed gasification with hot-gas filtration and catalytic conversion [33]. Pressure drop alone is insufficient to validate reactive mixing; temperature, solids distribution, residence time and species measurements provide complementary constraints.

6.6 Cross-study findings and unresolved questions

The evidence map points to recurring gaps: inconsistent product lumps, limited property data for softened mixed plastics, weak separation of calibration and validation, incomplete reporting of closures, and few public cases that combine experiments with executable model inputs. These gaps guide the open and reproducible workflow developed in the following chapters. Catalyst studies further show that coke may be a deactivation mechanism, a gasifiable reactant or a valuable carbon product depending on system design [10, 12, 17, 18]; models must therefore state their carbon objective and boundary explicitly.

Chapter 7

Open modelling tools

7.1 Selection criteria

Tools are assessed against openness of source and equations, licence conditions, reacting and multiphase capability, parallel scalability, extensibility, verification resources, interoperability, documentation and the ability to preserve an executable research record.

7.2 Thermochemistry and reacting systems

7.2.1 Cantera

Cantera provides open thermodynamics, chemical kinetics, transport and zero-dimensional reactor networks with Python and compiled-language interfaces [38]. It is well suited to equilibrium bounds, gas-phase kinetic calculations, ideal-reactor baselines and reaction sensitivity studies. Its reactor networks use SUNDIALS integrators for stiff ODE and DAE systems, and sparse preconditioning supports larger chemical mechanisms.

7.2.2 Combustion Toolbox and complementary equilibrium tools

Combustion Toolbox provides an open implementation for gas- and condensed-phase thermochemical equilibrium problems [39]. Independent tools are valuable for cross-checking equilibrium calculations and exposing differences in species sets, databases and phase assumptions.

7.3 Continuum CFD

7.3.1 OpenFOAM

OpenFOAM provides an extensible finite-volume framework with reacting, multiphase, particle and parallel-computing capabilities. For HyWay, its main value is transparent implementation of conservation equations and closures, plus the ability to add plastic-specific source terms. This flexibility also places responsibility on the modeller to document the selected distribution, version, solver, modifications and parallel-output strategy [40].

7.3.2 MFiX

NETL's MFiX suite includes two-fluid, DEM, coarse-grained DEM and PIC approaches for reacting gas–solid systems [41]. Its established multiphase closures and reactor focus make it a strong candidate for fluidised-bed studies and for comparisons between fidelity levels.

7.4 Numerical and data-analysis ecosystem

7.4.1 Python scientific stack

NumPy, SciPy, pandas, xarray, matplotlib and Jupyter support parameter estimation, uncertainty analysis, automated case generation and provenance. Python scripts should be treated as tested analysis software rather than as unrecorded interactive calculations.

7.4.2 PETSc and SUNDIALS

PETSc supplies scalable linear and nonlinear solvers, time integrators and optimisation infrastructure for parallel applications [42]. SUNDIALS supplies robust solvers for stiff ODEs, DAEs and nonlinear systems. These libraries are important both directly and as numerical foundations beneath higher-level modelling tools.

7.5 Workflow, meshing and post-processing tools

Gmsh, ParaView, mesh-quality utilities and version-controlled case-generation scripts complete the workflow. Open licensing alone does not ensure reproducibility: versions, compilation options, input data and post-processing definitions must be captured together.

7.6 Tool comparison

Table 7.1: Indicative roles of open tools in the HyWay model hierarchy.

Tool	Primary role	Strength for this report	Main caution
Cantera	Thermochemistry, kinetics, ideal reactors	Transparent mechanisms and rapid parameter studies	Polymer devolatilisation requires a suitable reduced or custom representation
OpenFOAM	Finite-volume CFD	Extensible reacting-flow and multiphase framework; MPI parallelism	Version and solver choices must be explicit; custom models require verification
MFiX	Reacting multiphase CFD, DEM and PIC	Multiple gas–solid fidelity levels in one ecosystem	Industrial-scale particle models can be computationally intensive
PETSc	Scalable numerical solvers	Parallel linear, nonlinear, transient and optimisation capability	Usually a building block rather than a complete process model
SUNDIALS	Stiff integration and nonlinear solution	Appropriate for chemical reactor networks and sensitivities	Performance depends on Jacobians, tolerances and preconditioning
Python stack	Orchestration, fitting and analysis	Reproducible automation and broad data ecosystem	Environments and random seeds must be locked and recorded
Gmsh/ParaView	Meshing and visualisation	Scriptable geometry and open post-processing	Visual agreement is not quantitative validation

Chapter 8

Open equilibrium simulation case study

8.1 Purpose and research questions

An open, reproducible Cantera study was conducted to turn the review findings into an executable baseline. The calculation asks three deliberately limited questions: how equilibrium hydrogen yield changes with temperature, steam and pressure; how idealised polymer composition changes the thermodynamic bound; and where solid-carbon formation remains favourable. It does not claim to predict a real reactor. Equilibrium screening is appropriate at this stage because published process models repeatedly use equilibrium or quasi-equilibrium calculations for sensitivity and flowsheet design [25, 28–30], while the experimental literature identifies feed, temperature and steam as central variables [7, 24, 26].

8.2 Model formulation

The model uses Cantera 3.2.0 [38], the GRI-Mech 3.0 thermochemical species set supplied as `gri30.yaml`, and the Cantera graphite phase. Each calculation minimises Gibbs free energy at fixed temperature and pressure using Cantera's VCS solver, with a freshly initialised Gibbs-solver fallback. Feed inputs are normalised to one mole of feed carbon. The idealised empirical units are CH_2 for PE/PP-like material, CH for PS-like material, and $CH_{0.8}O_{0.4}$ for PET-like material. The mixed feed assigns 70, 20 and 10% of feed carbon to those components, respectively. These are elemental screening representations, not polymer devolatilisation mechanisms.

Table 8.1: Design of the Cantera equilibrium parameter sweep.

Factor	Values	Count
Feed	PE/PP-like, PS-like, PET-like, mixed	4
Temperature	600–1100 °C in 10 °C increments	51
Steam-to-carbon ratio	0.5–4.0 in increments of 0.1	36
Pressure	1, 2, 5, 10, 20 and 30 bar	6
Total	Full factorial design	44,064

Outputs include H_2, CO, CO_2 and CH_4 yields per mole of feed carbon, dry H_2 mole fraction, H_2/CO ratio, solid carbon and carbon conversion. Hydrogen mass yield is normalised to the dry idealised feed; steam is excluded from that denominator. Consequently, increasing S/C is not cost-free even when the reported feed-normalised hydrogen yield rises.

8.3 HPC workflow and verification

The 44,064 cases were bundled into 111 chunks of up to 400 cases and executed as a Slurm array on the University of Luxembourg Aion HPC system, with at most four one-CPU tasks active concurrently. This ensemble structure used HPC where it was scientifically useful—to evaluate a dense full-factorial grid—while avoiding unnecessary parallelism within each inexpensive equilibrium solve. A dependent batch step merged, checked and plotted the results. The environment contained Python 3.12.13 and Cantera 3.2.0 on x86-64 Linux. All 44,064 cases converged; the largest relative elemental balance error across C, H and O was 6.24×10^{-11}. All model inputs, environment specifications, Slurm scripts, raw and merged outputs, analysis code, figures and tables needed to reproduce the study are included in the Zenodo repository 10.5281/zenodo.2172194.

8.4 Effects of steam and temperature

Figure 8.1 shows the mixed-feed response at 1 bar. Increasing steam raises the hydrogen bound throughout the grid and suppresses solid carbon. At low S/C, increasing temperature is required to cross the 90 and 99% carbon-conversion contours. At high S/C, hydrogen yield exhibits a broad maximum at intermediate temperature: low temperature favours water–gas shift, whereas high temperature progressively lowers the equilibrium H_2/CO ratio. The sampled-grid maximum, marked in the figure, is 2.409 mol H_2 mol^{-1} feed C at 670 °C, 1 bar and S/C=4. This boundary maximum should be read as a screening result; an energy and water penalty is absent from the objective.

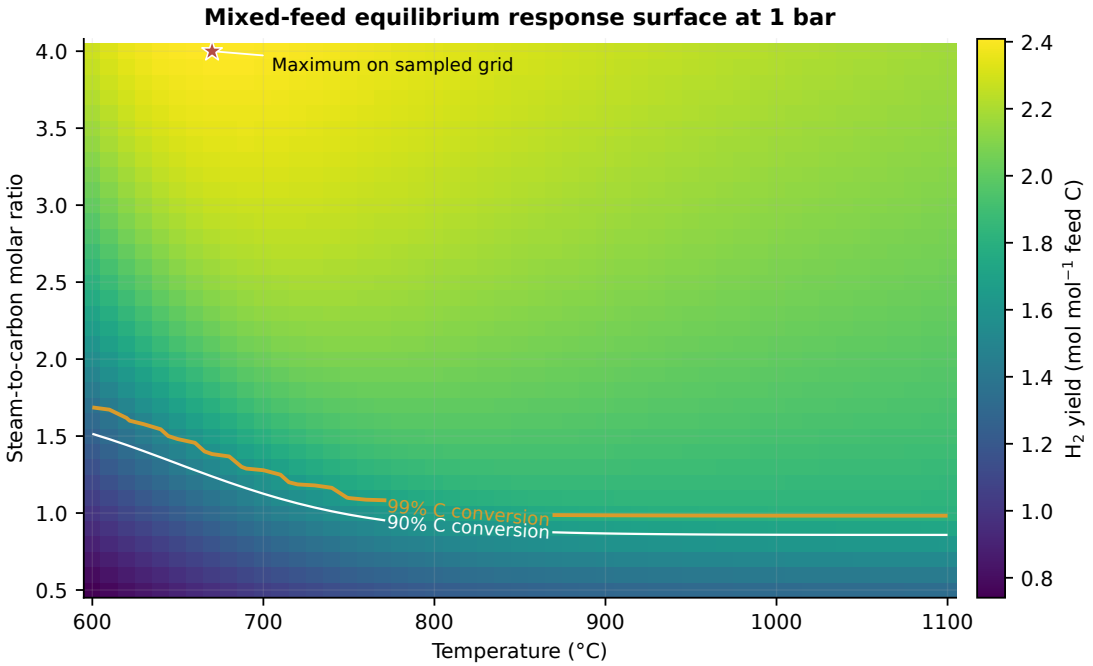

Figure 8.1: Equilibrium hydrogen response surface for the idealised mixed feed at 1 bar. Contours mark 90 and 99% carbon conversion; the star is the maximum on the sampled grid.

The steam response in Figure 8.2 is monotonic over the sampled interval, but its temperature ordering changes. At S/C below about 1.3, 900–1000 °C is beneficial because carbon conversion and methane reforming constrain H_2. At higher steam, 700–800 °C gives the larger equilibrium H_2 yield. This crossover is precisely why a single "higher temperature is better" statement is not defensible without fixing steam input and the performance metric.

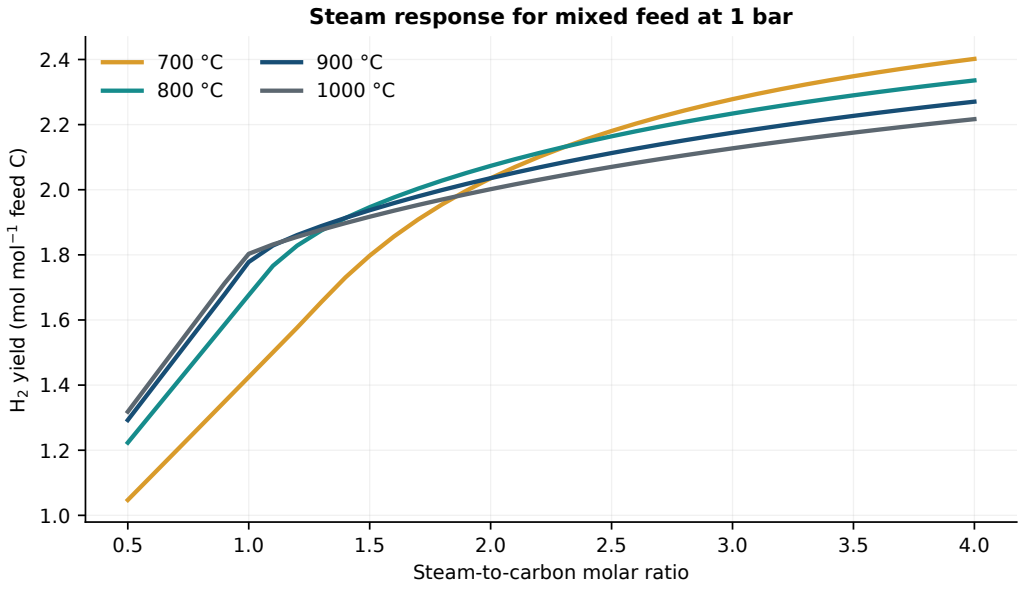

Figure 8.2: Effect of steam-to-carbon ratio on mixed-feed equilibrium hydrogen yield at 1 bar.

8.5 Feed-composition effects

At 1 bar and S/C=2, the PE/PP-like feed has the highest molar and mass-based hydrogen bounds, the mixed feed is intermediate, and PET-like feed is lowest (Figure 8.3). This ordering follows the feed hydrogen and oxygen inventories and is directionally consistent with polymer-resolved reforming experiments [7–9]. It is not an experimental validation: the model omits polymer-specific volatile distributions, tar and catalyst reactivity that contribute to the observed ranking.

At S/C=1, carbon conversion is strongly feed dependent. The minimum temperature for 99% conversion at 1 bar is 690 °C for PET-like feed, 820 °C for the mixed feed, 890 °C for PE/PP-like feed and 920 °C for PS-like feed. At 30 bar the corresponding thresholds rise to 860, 950, 960 and 1050 °C. The PS result reinforces the experimental warning that aromatic feed behaviour should not be inferred from a polyolefin model [6, 7].

Table 8.2: Maximum equilibrium hydrogen yield for each feed on the sampled grid.

Feed	T (°C)	P (bar)	S/C	mol H_2/mol C	kg H_2/kg feed
PE/PP-like	680	1	4.0	2.583	0.371
PS-like	660	1	4.0	2.139	0.331
PET-like	640	1	4.0	1.737	0.182
Mixed	670	1	4.0	2.409	0.338

8.6 Pressure effects

Pressure favours methane relative to the higher-mole-number reforming products, so its hydrogen penalty is most pronounced at lower temperature (Figure 8.4). For mixed feed at S/C=2 and 700 °C, increasing pressure from 1 to 30 bar lowers the equilibrium H_2 yield from 2.035 to 0.752 mol mol^{-1} feed C while increasing residual CH_4 from 0.039 to 0.474 mol mol^{-1} feed C. At 900 °C, the H_2 yield decreases from 2.036 to 1.646 over the same pressure interval; by 1100 °C the curves

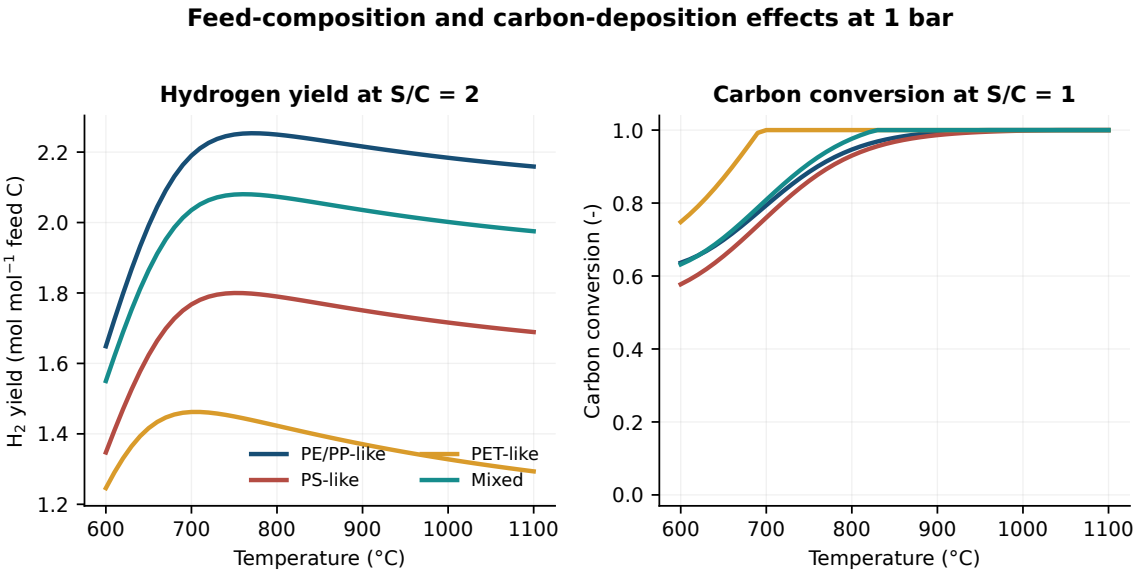

Figure 8.3: Idealised feed-composition effects at 1 bar: hydrogen yield at S/C=2 (left) and carbon conversion at S/C=1 (right).

nearly converge as methane becomes small. These results identify a clear screening trade-off between low-pressure reforming and any downstream benefit of delivering pressurised gas.

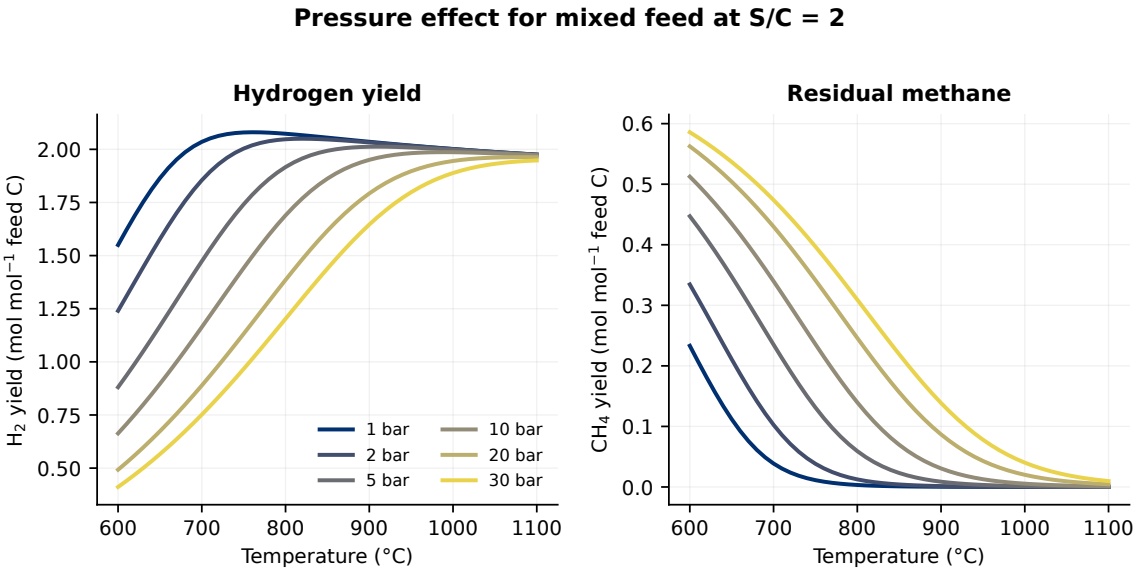

Figure 8.4: Pressure effect on equilibrium hydrogen and residual methane for the idealised mixed feed at S/C=2.

8.7 Interpretation and limitations

The study provides a verified thermodynamic envelope, not a reactor prediction. It assumes instantaneous equilibrium, a restricted gas species set, ideal-gas behaviour and graphite as the only condensed carbon phase. It does not represent polymer melting or devolatilisation, finite residence time, tar, catalyst activity and deactivation, heat duty, steam generation, separation, pressure work, contaminants or real mixture variability. The apparent optima therefore cannot be

used as operating set points. Their value is to reject thermodynamically poor regions, initialise richer models and define focused experimental comparisons.

The next model level should replace the empirical feed units with measured or kinetically predicted pyrolysis volatile distributions and couple them to a lumped reformer with catalyst deactivation, following the evidence in Cortazar et al. [25] and Barbarias et al. [20]. Validation should use polymer-resolved gas yields and composition from continuous two-stage studies [7], with carbon closure retained explicitly when chars or ashes participate [15, 24].

Chapter 9

Recommendations and next steps

9.1 Modelling and validation strategy

HyWay should retain a staged hierarchy in which model complexity follows the available evidence. The Cantera study in Chapter 8 supplies a verified thermodynamic envelope and a reproducible parameter grid. Its carbon-conversion contours can narrow the experimental and kinetic-model domain, but they are not validation data. The next level should couple polymer-resolved or measured pyrolysis volatile distributions to a lumped finite-rate reformer that includes methane, light and heavy hydrocarbons, water–gas shift and catalyst deactivation. Reactor-scale CFD should be reserved for questions in which heat transfer, mixing or residence time materially change the result; particle methods should be introduced only where continuum descriptions cannot represent the observed hydrodynamics.

Verification should continue to begin with conservation, solver-tolerance and time-step or mesh checks. Validation should use measurements not employed for calibration and should compare several observables—for example conversion, gas yield, dry gas composition, carbon deposition and temperature—rather than only outlet hydrogen. The present calculation passed its numerical checks, but remains an unvalidated equilibrium screening model. Feed composition, kinetic and property parameters, boundary conditions and multiphase closures should be treated as uncertain wherever later models depend on them.

9.2 Research priorities and reproducibility

The literature remains limited by inconsistent product definitions, variable mixed-waste composition, uncertain properties of softened plastics and a shortage of independent reactor-scale validation data. Although many studies use proprietary flowsheets or bespoke fitted models, few provide executable case files, which restricts direct reproduction. Immediate priorities are therefore to standardise feed and product definitions, validate selected baseline cases and establish polymer-resolved volatile inputs. The equilibrium sweep indicates that low pressure is thermodynamically favourable for H_2, steam suppresses solid carbon, and feed identity changes both yield and the temperature required for conversion. Heat duty, water use, compression, kinetics, tar and catalyst stability must be added before optimisation.

This final report and the complete computational record are deposited in the Zenodo archive 10.5281/zenodo.2172194. The archive contains the report, source code, environment definition, local and HPC instructions, Slurm scripts, raw and merged results, figures, tables and a file-by-file reproduction guide. It therefore provides the executable baseline from which kinetic, uncertainty and reactor-scale extensions can be developed.

Chapter 10

Conclusions

Plastic-to-hydrogen modelling requires a hierarchy rather than a single all-purpose simulation. Thermodynamic calculations define limits; kinetic and ideal-reactor models establish interpretable baselines; CFD resolves transport and hydrodynamics; and particle or multiscale approaches target specific closure questions. Open tools make this hierarchy inspectable and executable on HPC facilities, while reproducible workflows preserve the connection between data, assumptions and reported conclusions.

The literature synthesis shows that polymer-specific volatile production, finite-rate reforming, catalyst deactivation and carbon accounting are the most reusable links between experiments and model development. The open Aion study adds a verified thermodynamic envelope: across 44,064 cases, hydrogen is favoured by lower pressure and adequate steam, while feed composition changes the attainable yield and carbon-conversion threshold. For the idealised mixed feed, the sampled maximum is 2.409 mol H_2 per mol feed carbon at 670 °C, 1 bar and S/C=4. Because energy, kinetics, tar and real-feed variability are absent, this value is an upper bound rather than a proposed operating condition. The next defensible step is experimental validation of a finite-rate pyrolysis–reforming network within the same reproducible model hierarchy. The report, model and complete computational record are available from 10.5281/zenodo.2172194.

Bibliography

[1] Hamad Hussain Shah, Muhammad Amin, Amjad Iqbal, Irfan Nadeem, Mitjan Kalin, Arsalan Muhammad Soomar, and Ahmed M. Galal. A review on gasification and pyrolysis of waste plastics. *Frontiers in Chemistry*, 10:960894, 2023. doi: 10.3389/fchem.2022.960894.

[2] S. M. Al-Salem and Paola Lettieri. Kinetic study of high density polyethylene (HDPE) pyrolysis. *Chemical Engineering Research and Design*, 88(12):1599–1606, 2010. doi: 10.1016/j.cherd.2010.03.012.

[3] Haoyu Li, Ondřej Mašek, Alan Harper, and Raffaella Ocone. Kinetic study of pyrolysis of high-density polyethylene (HDPE) waste at different bed thickness in a fixed bed reactor. *The Canadian Journal of Chemical Engineering*, 99(8):1733–1744, 2021. doi: 10.1002/cjce.24123.

[4] Ibrahim Dubdub and Mohammed Al-Yaari. Pyrolysis of low density polyethylene: Kinetic study using TGA data and ANN prediction. *Polymers*, 12(4):891, 2020. doi: 10.3390/polym12040891.

[5] Fatemeh Vatankhah, Abdelkader Kara, Adrián Carrillo García, and Jamal Chaouki. Kinetic modeling of polyethylene pyrolysis under microwave irradiation toward predictive product distribution. *Chemical Engineering Journal*, 525:170441, 2025. doi: 10.1016/j.cej.2025.170441.

[6] Tomoaki Namioka, Atsushi Saito, Yukiharu Inoue, Yeongsu Park, Taijin Min, Seon Ah Roh, and Kunio Yoshikawa. Hydrogen-rich gas production from waste plastics by pyrolysis and low-temperature steam reforming over a ruthenium catalyst. *Applied Energy*, 88(6):2019–2026, 2011. doi: 10.1016/j.apenergy.2010.12.053.

[7] Itsaso Barbarias, Gartzen López, Maite Artetxe, Aitor Arregi, Javier Bilbao, and Martín Olazar. Valorisation of different waste plastics by pyrolysis and in-line catalytic steam reforming for hydrogen production. *Energy Conversion and Management*, 156:575–584, 2018. doi: 10.1016/j.enconman.2017.11.048.

[8] Idris Aminu, Mohamad A. Nahil, and Paul T. Williams. Pyrolysis-plasma/catalytic reforming of post-consumer waste plastics for hydrogen production. *Catalysis Today*, 420:114084, 2023. doi: 10.1016/j.cattod.2023.114084.

[9] Yukun Li, Mohamad A. Nahil, and Paul T. Williams. Hydrogen/syngas production from different types of waste plastics using a sacrificial tire char catalyst via pyrolysis–catalytic steam reforming. *Energy & Fuels*, 37(9):6661–6673, 2023. doi: 10.1021/acs.energyfuels.3c00499.

[10] Dingding Yao, Haiping Yang, Hanping Chen, and Paul T. Williams. Co-precipitation, impregnation and sol-gel preparation of Ni catalysts for pyrolysis-catalytic steam reforming of waste plastics. *Applied Catalysis B: Environmental*, 239:565–577, 2018. doi: 10.1016/j.apcatb.2018.07.075.

[11] Dingding Yao, Haiping Yang, Hanping Chen, and Paul T. Williams. Investigation of nickel-impregnated zeolite catalysts for hydrogen/syngas production from the catalytic reforming of waste polyethylene. *Applied Catalysis B: Environmental*, 227:477–487, 2018. doi: 10.1016/j.apcatb.2018.01.050.

[12] Ye Shui Zhang, Jun Huang, and Paul T. Williams. Fe–Ni–MCM-41 catalysts for hydrogen-rich syngas production from waste plastics by pyrolysis–catalytic steam reforming. *Energy & Fuels*, 31(8):8497–8504, 2017. doi: 10.1021/acs.energyfuels.7b01368.

[13] Ashiq Ahamed, Lili Liang, Wei Ping Chan, Preston Tan, Nicklaus Tze Xuan Yip, Johan Bobacka, Andrei Veksha, Ke Yin, and Grzegorz Lisak. In situ catalytic reforming of plastic pyrolysis vapors using MSW incineration ashes. *Environmental Pollution*, 276:116681, 2021. doi: 10.1016/j.envpol.2021.116681.

[14] Yukun Li and Paul T. Williams. Catalytic biochar and refuse-derived char for the steam reforming of waste plastics pyrolysis volatiles for hydrogen-rich syngas. *Industrial & Engineering Chemistry Research*, 62(36):14335–14348, 2023. doi: 10.1021/acs.iecr.3c02292.

[15] Yukun Li and Paul T. Williams. Waste derived ash as catalysts for the pyrolysis-catalytic steam reforming of waste plastics for hydrogen-rich syngas production. *Journal of Analytical and Applied Pyrolysis*, 177:106374, 2024. doi: 10.1016/j.jaap.2024.106374.

[16] Kevin M. Wyss, Karla J. Silva, Ksenia V. Bets, Wala A. Algozeeb, Carter Kittrell, Carolyn Teng, Chi Hun Choi, Weiyin Chen, Jacob L. Beckham, Boris I. Yakobson, and James M. Tour. Synthesis of clean hydrogen gas from waste plastic at zero net cost. *Advanced Materials*, 35(48):2306763, 2023. doi: 10.1002/adma.202306763.

[17] Jonathan C. Acomb, Chunfei Wu, and Paul T. Williams. Control of steam input to the pyrolysis-gasification of waste plastics for improved production of hydrogen or carbon nanotubes. *Applied Catalysis B: Environmental*, 147:571–584, 2013. doi: 10.1016/j.apcatb.2013.09.018.

[18] Chunfei Wu, Mohamad A. Nahil, Norbert Miskolczi, Jun Huang, and Paul T. Williams. Production and application of carbon nanotubes, as a co-product of hydrogen from the pyrolysis-catalytic reforming of waste plastic. *Process Safety and Environmental Protection*, 103:107–114, 2016. doi: 10.1016/j.psep.2016.07.001.

[19] Aitor Arregi, Maider Amutio, Gartzen López, Maite Artetxe, Jon Álvarez, Javier Bilbao, and Martín Olazar. Hydrogen-rich gas production by continuous pyrolysis and in-line catalytic reforming of pine wood waste and HDPE mixtures. *Energy Conversion and Management*, 136:192–201, 2017. doi: 10.1016/j.enconman.2017.01.008.

[20] Itsaso Barbarias, Gartzen López, Maite Artetxe, Aitor Arregi, Javier Bilbao, and Martín Olazar. Kinetic modeling of the catalytic steam reforming of high-density polyethylene pyrolysis volatiles. *Energy & Fuels*, 31(11):12645–12653, 2017. doi: 10.1021/acs.energyfuels.7b01909.

[21] Idris Aminu, Mohamad A. Nahil, and Paul T. Williams. Hydrogen from waste plastics by two-stage pyrolysis/low-temperature plasma catalytic processing. *Energy & Fuels*, 34(9):11679–11689, 2020. doi: 10.1021/acs.energyfuels.0c02043.

[22] Idris Aminu, Mohamad A. Nahil, and Paul T. Williams. Hydrogen production by pyrolysis–nonthermal plasma/catalytic reforming of waste plastic over different catalyst support materials. *Energy & Fuels*, 36(7):3788–3801, 2022. doi: 10.1021/acs.energyfuels.1c04186.

[23] Mengmeng Du, Yu Zhang, Sailei Kang, Xuyun Guo, Yingxin Ma, Mengyuan Xing, Ye Zhu, Yang Chai, and Bocheng Qiu. Trash to treasure: Photoreforming of plastic waste into commodity chemicals and hydrogen over MoS2-tipped CdS nanorods. *ACS Catalysis*, 12 (20):12823–12832, 2022. doi: 10.1021/acscatal.2c03605.

[24] Yukun Li, Mohamad A. Nahil, and Paul T. Williams. Pyrolysis-catalytic steam reforming of waste plastics for enhanced hydrogen/syngas yield using sacrificial tire pyrolysis char catalyst. *Chemical Engineering Journal*, 467:143427, 2023. doi: 10.1016/j.cej.2023.143427.

[25] María Cortazar, Ningbo Gao, Cui Quan, Mayra Alejandra Suarez, Gartzen López, Santiago Orozco, Laura Santamaria, Maider Amutio, and Martín Olazar. Analysis of hydrogen production potential from waste plastics by pyrolysis and in line oxidative steam reforming. *Fuel Processing Technology*, 225:107044, 2022. doi: 10.1016/j.fuproc.2021.107044.

[26] Danbee Han, Seungcheol Shin, Haneul Jung, Wonjun Cho, and Youngsoon Baek. Hydrogen production by steam reforming of pyrolysis oil from waste plastic over 3 wt.% Ni/Ce-Zr-Mg/Al2O3 catalyst. *Energies*, 16(6):2656, 2023. doi: 10.3390/en16062656.

[27] Yesol Woo, Jae Min Park, Jong Wook Bae, and Myung-June Park. Kinetic modeling of the steam reforming of light hydrocarbon mixture from waste resources: Effects of gas composition on hydrogen production. *International Journal of Hydrogen Energy*, 48(41): 15383–15391, 2023. doi: 10.1016/j.ijhydene.2023.01.050.

[28] Ali A. Al-Qadri, Usama Ahmed, Abdul Gani Abdul Jameel, Umer Zahid, Muhammad Usman, and Nabeel Ahmad. Simulation and modelling of hydrogen production from waste plastics: Technoeconomic analysis. *Polymers*, 14(10):2056, 2022. doi: 10.3390/polym14102056.

[29] Mohammad Lahafdoozian, Hossein Khoshkroudmansouri, Sharif H. Zein, and Aishah Abdul Jalil. Hydrogen production from plastic waste: A comprehensive simulation and machine learning study. *International Journal of Hydrogen Energy*, 59:465–479, 2024. doi: 10.1016/j.ijhydene.2024.01.326.

[30] Nishant Ranjan, Narendra Yadav, Harmanpreet Singh, Sandeep Kumar, and Sanjay M. Mahajani. Modelling and simulation of autothermal downdraft co-gasification of biomass and plastic wastes using Aspen Plus. *Energy Conversion and Management*, 297:117714, 2023. doi: 10.1016/j.enconman.2023.117714.

[31] Mohamed Ismail and İbrahim Dinçer. A new renewable energy based integrated gasification system for hydrogen production from plastic wastes. *Energy*, 270:126869, 2023. doi: 10.1016/j.energy.2023.126869.

[32] Patient E. Ganza and BongJu Lee. A novel method for industrial production of clean hydrogen (H2) from mixed plastic waste. *International Journal of Hydrogen Energy*, 48(40): 15037–15052, 2023. doi: 10.1016/j.ijhydene.2023.01.010.

[33] Armando Vitale, Alessandro Antonio Papa, Andrea Di Carlo, and Sergio Rapagnà. Plastic waste gasification to synthetic natural gas: experimental catalytic steam gasification and methanation process modelling in Aspen Plus. *Waste Management*, 222:115631, 2026. doi: 10.1016/j.wasman.2026.115631.

[34] Kai Lan and Yuan Yao. Feasibility of gasifying mixed plastic waste for hydrogen production and carbon capture and storage. *Communications Earth & Environment*, 3(1):300, 2022. doi: 10.1038/s43247-022-00632-1.

[35] Shaik Afzal, Avantika Singh, Scott Nicholson, Taylor Uekert, Jason S. DesVeaux, Eric C. D. Tan, Abhijit Dutta, Alberta Carpenter, R. M. Baldwin, and Gregg T. Beckham.

Techno-economic analysis and life cycle assessment of mixed plastic waste gasification for production of methanol and hydrogen. *Green Chemistry*, 25(13):5068–5085, 2023. doi: 10.1039/d3gc00679d.

[36] Suviti Chari, Alex Sebastiani, Andrea Paulillo, and Massimiliano Materazzi. The environmental performance of mixed plastic waste gasification with carbon capture and storage to produce hydrogen in the U.K. *ACS Sustainable Chemistry & Engineering*, 11(8):3248–3259, 2023. doi: 10.1021/acssuschemeng.2c05978.

[37] Weiwei Xuan, Hailun Wang, Shuo Yan, and Dehong Xia. Exploration on the steam gasification mechanism of waste PE plastics based on ReaxFF-MD and DFT methods. *Fuel*, 315:123121, 2022. doi: 10.1016/j.fuel.2021.123121.

[38] Cantera Developers. Cantera: Open-source chemical kinetics, thermodynamics, and transport. https://cantera.org/, 2026. Accessed 31 July 2026.

[39] Alberto Cuadra, César Huete, and Marcos Vera. Combustion toolbox: An open-source thermochemical code for gas- and condensed-phase problems involving chemical equilibrium. *arXiv preprint arXiv:2409.15086*, 2024. doi: 10.48550/arXiv.2409.15086.

[40] OpenFOAM Foundation. OpenFOAM parallel i/o. https://openfoam.org/guides/parallel-io/, 2017. Accessed 31 July 2026.

[41] National Energy Technology Laboratory. MFiX: Open-source multiphase flow modelling for real-world applications. https://mfix.netl.doe.gov/products/mfix/, 2026. Accessed 31 July 2026.

[42] PETSc Development Team. PETSc: Portable, extensible toolkit for scientific computation. https://petsc.org/release/, 2026. Accessed 31 July 2026.